Available online at www.sciencedirect.com

SCIENCE DIRECT

Thin Solid Films 488 (2005) 34 – 39

www.elsevier.com/locate/tsf

Preparation and characterization of molecular-material thin films containing diaqua tetrabenzo (*b*,*f*,*j*,*n*) {1,5,9,13} tetraazacyclohexadecine copper (II) and nickel (II) bisanthraflavates

M.E. Sánchez-Vergara[a,*], A. Ortiz[b], Cecilio Álvarez-Toledano[c], J.R. Alvarez[a]

[a]*Instituto Tecnológico y de Estudios Superiores de Monterrey, Campus Ciudad de México, Calle del Puente 222, Col. Ejidos de Huipulco, 14380, México, D.F.*
[b]*Instituto de Investigaciones en Materiales, Universidad Nacional Autónoma de México, A.P. 70-360, Coyoacán, 04510, México, D.F.*
[c]*Instituto de Química, Universidad Nacional Autónoma de México, Circuito Exterior, Ciudad Universitaria, 04510, México, D.F.*

Received 13 February 2004; received in revised form 14 December 2004; accepted 5 April 2005
Available online 2 June 2005

Abstract

Semiconducting molecular-material thin films of tetrabenzo (*b*,*f*,*j*,*n*) {1,5,9,13} tetraazacyclohexadecine copper (II) and nickel (II) bisanthraflavates have been prepared by using vacuum thermal evaporation on corning glass substrates and crystalline silicon wafers. The obtained films were characterized by infrared spectroscopy (FTIR), atomic force microscopy (AFM), ultraviolet-visible (UV-Vis) spectroscopy and ellipsometry. The values of the electric current as a function of temperature are always higher for the complexes with nickel than for those with copper. Charge transfer for these complexes shows preferential conducting paths that can be attributed to the hydrogen bonds of the anthraflavate anions. Electric conductivity values found for thin films are higher than for pellets made of the same molecular materials.

PACS: A; E
Keywords: Anisotropy; Conductivity; Electrical properties and measurements; Organic semiconductors

1. Introduction

There has been an increasing interest on molecular materials over the last years because of their electric, magnetic and/or optical properties, which may lead to electronic device applications [1,2]. Recent research work has been oriented to the formation and characterization of molecular-material thin films [3]. The use of chemical vapour deposition to grow thin films of molecular conductors such as tetrathiafulvalene–tetracyanoqunodimethane (TTF–TCNQ) has been reported [4–6]. TTF–TCNQ is considered the first real organic metal [7,8]. Its highly anisotropic conductivity almost reaches metallic values along a preferred direction defined by its structural configuration. This arises from a great number of long and parallel chains or molecular stacks along which conduction seems to occur.

A regular stacking of molecules such as is found in molecular materials may permit the formation of semiconducting, conducting or superconducting thin films. Metallophthalocyanines (MPcs), for example, have been extensively studied due to their electrical properties and their ability to form good-quality thin films. MPcs thin films are of particular interest in the study of low-dimensional metals and semiconductors as one may bridge metallophthalocyanine nuclei with linear bidentate axial ligands, which suggests a model for low-dimensional polymeric conduction in macrocycles. In these ligand-bridged systems, the central metal-axial ligand spine is expected to be a reasonable pathway for conduction [9]. Special attention must be given to ligand-bridged materials with a highly delocalized electronic structure such as macrocycle complexes that have been used as models for the construction of

* Corresponding author. Tel.: +52 55 5483 2199; fax: +52 55 5483 2163.
E-mail address: mesv@itesm.mx (M.E. Sánchez-Vergara).

0040-6090/$ - see front matter © 2005 Elsevier B.V. All rights reserved.
doi:10.1016/j.tsf.2005.04.087

conductive materials [10,11]. The tetrabenzo (*b*,*f*,*j*,*n*) {1,5,9,13} tetraazacyclohexadecine metal (II) complex is one of the macrocycles employed for that purpose in this work [12]. These materials may show interesting changes in their electric conductivity when incorporating substitute groups to their macrocyclic ligands.

In this paper, we report the preparation and characterization of molecular-material thin films containing diaqua tetrabenzo (*b*,*f*,*j*,*n*) {1,5,9,13} tetraazacyclohexadecine copper (II) and nickel (II) bisanthraflavates prepared by thermal evaporation. Electric conductivity results from thin films are compared with those obtained by pellet measurements for the same materials $[M(TAAB)(H_2O)_2](C_{14}H_7O_4)_2$ (M=Ni,Cu), formed under high-pressure conditions.

2. Experiments

2.1. Starting material and chemicals

Reagent-grade commercial products were used without further purification except for the *o*-aminobenzaldehyde complex which was prepared according to Smith [13] from heptahydrated ferrous sulphate and orthonitrobenzaldehyde. Perchlorate of [tetrabenzo (*b*,*f*,*j*,*n*) {1,5,9,13} tetraazacyclohexadecine] nickel (II): $[Ni(TAAB)(H_2O)_2](ClO_4)_2$ and nitrate of [tetrabenzo (*b*,*f*,*j*,*n*) {1,5,9,13} tetraazacyclohexadecine] copper (II): $[Cu(TAAB)(H_2O)_2](NO_3)_2$ macrocycles were prepared according to literature [14]. Diaqua tetrabenzo (*b*,*f*,*j*,*n*) {1,5,9,13} tetraazacyclohexadecine nickel (II) and copper (II) bisanthraflavates ($[Ni(TAAB)(H_2O)_2](C_{14}H_7O_4)_2$, $[Cu(TAAB)(H_2O)_2](C_{14}H_7O_4)_2$) were previously reported by some of the authors of this paper [15]. In this case, anthraflavic acid was used instead of a potassium double salt in order to generate a double substitution between the acid and the complex.

2.2. Synthesis of $[Ni(TAAB)(H_2O)_2](C_{14}H_7O_4)_2$

0.37g (0.06 mmol) of $[Ni(TAAB)(H_2O)_2](ClO_4)_2$ in 15 ml absolute ethanol was added to 0.36 g (1.2 mmol) of anthraflavic acid previously dissolved in 10 ml of absolute ethanol. The resulting solution was refluxed for 2 days until a red precipitate appeared. The solid was filtered off, washed with absolute ethanol and dried vacuum. The product was recrystallized in a 1:1 ethanol–water solution. Yield 68% (0.4 g). (Found: C, 68.42; H, 3.72; N, 5.57. Calcd.: 68.22; H, 3.85; N, 5.69).

2.3. Synthesis of $[Cu(TAAB)(H_2O)_2](C_{14}H_7O_4)_2$

0.2 g (0.64 mmol) of anthraflavic acid previously dissolved in 20 ml of absolute methanol was added to 0.16 g (0.27 mmol) solution of $[Cu(TAAB)(H_2O)_2](NO_3)_2$ in 10 ml of absolute methanol. The resulting solution was refluxed for two days until an olive green precipitate appeared. The solid was filtered off, washed with absolute methanol and dried in vacuum. The product was recrystallized in a 1:1 methanol–water solution. Yield 71% (0.19 g). (Found: C, 67.13; H, 3.26; N, 5.38. Calcd.: C, 67.91; H, 3.84; N, 5.66).

2.4. Thin film deposition measurements

Thin film deposition of $[Ni(TAAB)(H_2O)_2](C_{14}H_7O_4)_2$ and $[Cu(TAAB)(H_2O)_2](C_{14}H_7O_4)_2$ was carried out by vacuum thermal evaporation onto Corning 7059 glass slices and (100) single-crystalline silicon (c-Si), 200 Ω-cm wafers. The substrates were kept at 298 K. The Corning 7059 substrates were ultrasonically degreased in warm ethanol and dried in a nitrogen atmosphere. The substrates underwent chemical etching with a p solution (10 ml HF, 15 ml HNO_3, 300 ml H_2O) in order to remove the native oxide from the c-Si surface. To prevent the power products from condensing on the surface of the substrate, the evaporation source was a molybdenum boat with two grids. The temperature in the boat was 453 K during evaporation, measured with a chromel–alumel thermocouple. It should be remarked that the synthesized compound sublimates. The temperature through the molybdenum boat was slowly increased to 453 K, below the first change observed in the thermo-gravimetric analysis thermogram, to prevent thermal decomposition of the compound.

2.5. Thin film characterization

The surface texture of deposited films was analyzed by means of atomic force microscopy (AFM) using a Digital Instruments, NanoScope IIIa microscope. Infrared spectra (FTIR) were recorded with a Nicolet 5-Mx FT-IR spectrophotometer with a resolution of 4 cm^{-1}. The refraction index and thickness of films were determined by ellipsometry using a Gaetner L117 variable-angle manual ellipsometer with a helium–neon laser as a light source (λ=632.8 nm, ∅=1 mm at 1 mW). The incidence angle was 70°. The infrared and ellipsometric measurements were carried out in the film deposited onto c-Si substrates. Ultraviolet-visible (UV-Vis) transmission and absorption spectra for films deposited onto naked Corning 7059 glass substrates were obtained with a Shimadzu 260 double-beam spectrophotometer. The optical absorption spectra of these samples were studied to evaluate the absorption coefficient, the optical gap and the nature of the electronic transitions involved. The electric conductivity of the films was studied by means of a four-point probe; for these measurements, the substrates were Corning 7059 glass slices coated with four metallic strips that acted as electrodes. The strips were deposited by thermal evaporation. In order to get an ohmic contact with the deposited films, the electrodes were made from gold or silver. Electric current as a function of temperature was measured with an applied voltage of 100 V in the ohmic regime, using a programmable voltage

source Keithley 230 and a peak-ammeter Keithley 485 coupled to an HP3421 data collector (for both pellets and thin films).

3. Results and discussion

AFM has been used independently to assess the surface quality of the thin films. Fig. 1 shows two-dimensional AFM images obtained from $[Ni(TAAB)(H_2O)_2](C_{14}H_7O_4)_2$ and $[Cu(TAAB)(H_2O)_2](C_{14}H_7O_4)_2$ thin films. The root mean square (r.m.s.) roughness evaluated from AFM measurement of the thin films is 40.5 nm for $[Ni(TAAB)(H_2O)_2](C_{14}H_7O_4)_2$ and 68.1 nm for $[Cu(TAAB)(H_2O)_2](C_{14}H_7O_4)_2$. The difference in roughness could be correlated with the molecular structure and the chemical composition. All thin-film surfaces show an amorphous character. The $[Ni(TAAB)(H_2O)_2](C_{14}H_7O_4)_2$ film is more uniformly distributed on the substrate surface and its final texture is not as grainy as in the other compound. The $[Cu(TAAB)(H_2O)_2](C_{14}H_7O_4)_2$ film shows a spotty granular texture on its surface. However, no pinholes were observed in analyzed films.

FTIR spectroscopic measurements on thin films were made to determine if there were significant changes in the raw materials after thermal evaporation. Table 1 shows the IR band spectra for the newly synthesized compounds in their different forms (powder and film). The IR spectra show that thin films have the same absorption bands as the powder used for evaporation. The slight shifts observed may be due to internal stress produced by the evaporation process. These results suggest that thermal evaporation is a molecular process that does not change the relative chemical composition of the synthesized compounds. The deposited films are formed by the same macro-ions as those of the original synthesized powder. The IR spectrum of the $[Ni(TAAB)(H_2O)_2](C_{14}H_7O_4)_2$ powder compound shows four absorption bands located at 1609, 1590, 1498 and 1447 cm^{-1} related to the stretching vibration of the ortho-disubstituted benzene radicals in the macrocycle. There is also a sharp, intense band at 1568 cm^{-1} associated to the C═N stretching vibration of the imine group. Finally, two more bands are found at 1309 and 1084 cm^{-1} corresponding to the C–O stretching vibration in anthraflavic acid. Just as for the IR spectrum of the nickel compound, several bands were found for the $[Cu(TAAB)(H_2O)_2](C_{14}H_7O_4)_2$ powder sample. Four of these bands are associated to the macrocycle ortho-disubstituted benzene fragments and another one is associated to the C═N stretching-mode vibration of the imine group, in addition to those bands associated to the C–O stretching-mode vibration in anthraflavic acid.

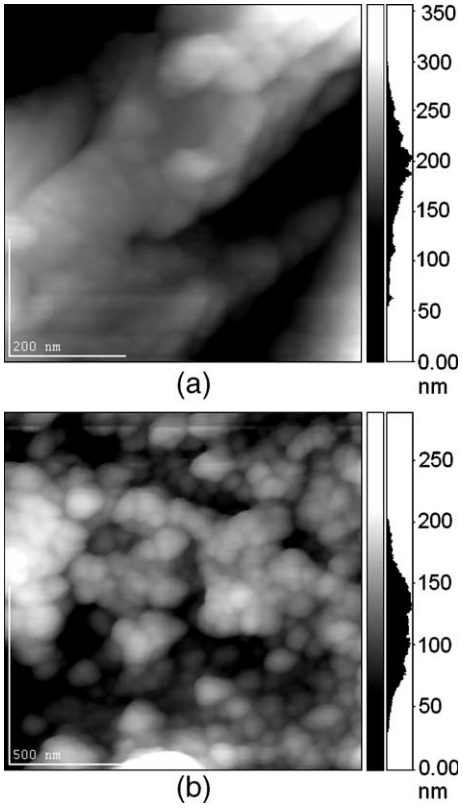

Fig. 1. AFM images of (a) $[Ni(TAAB)(H_2O)_2](ClO_4)_2$ and (b) $[Cu(TAAB)(H_2O)_2](NO_3)_2$.

From ellipsometry measurements, the approximate thickness of the deposited films studied is $t_h \sim 180$ nm. Refractive indices and absorption coefficients in semiconductors are relevant in the design and analysis of optoelectronic devices [16]. The refraction index and reflectance data of the thin films under study are shown in Table 2. The estimated reflectance for thin films is lower than 15%, so the optical properties of thin films can be analyzed according to the Tauc model [17], which was developed to study the optical properties of amorphous semiconductor materials.

The optical transmission and absorption spectra of these samples have been used to evaluate the absorption coefficient, optical gap and nature of the transitions involved [18]. The width of optical band gap E_g can be determined from straight-line interpolation in an $(\alpha h\nu)^{1/2}$ versus $(h\nu)$ plot. The absorption coefficient a near the band edge in many amorphous semiconductors shows an exponential dependence on photon energy usually obeying Urbach's empirical relation [19]:

$$\alpha h\nu = \beta\left(h\nu - E_g\right)^n \tag{1}$$

where β^{-1} is the band edge parameter, n is a number that characterizes the transition process, which takes values 1/2, 1, 3/2 or 2 depending on the nature of the electronic transitions responsible for the absorption [20]. One may recall here that, in amorphous semiconductors, optical transitions are described to a first approximation by non-direct transitions with no conservation of electronic momentum [21].

Table 1
IR data for the reported compounds in powder and thin films

Compound	ν (C═N)	ν (C_6 ring)	ν (C_6 ring)	ν (C_6 ring)	ν (C_6 ring)	ν (C–O)
$[Ni(TAAB)(H_2O)_2](C_{14}H_7O_4)_2$ (powder)	1568	1609	1590	1498	1447	1309,1084
$[Ni(TAAB)(H_2O)_2](C_{14}H_7O_4)_2$ (thin film)	1566	1610	1587	1491	1452	1317,1086
$[Cu(TAAB)(H_2O)_2](C_{14}H_7O_4)_2$ (powder)	1569	1614	1588	1496	1443	1305,1079
$[Cu(TAAB)(H_2O)_2](C_{14}H_7O_4)_2$ (thin film)	1568	1610	1589	1499	1448	1306,1081

All units cm^{-1}.

Fig. 2 shows the dependence of the absorption coefficient with photon energy. It can be observed that $[Ni(TAAB)(H_2O)_2](C_{14}H_7O_4)_2$ presents a lower absorption coefficient when compared with its starting material, while just the opposite occurs for the copper complexes.

The optical band gap energies, calculated from the Tauc model [17] using the results shown in Fig. 2, are provided in Table 2. These optical band gap values may be related to non-direct electronic interband transitions. An alternative explanation may be reached if one considers the generation of Frenkel-type, tightly-bound excitons [22]. It has been observed [23] that significant charge localization in organic molecular materials leads to a significant difference between the size of the optical gap and the size of the transport gap, which corresponds to the energy of formation of a separated free electron and a hole. Whereas the optical gap can be measured by optical absorption spectroscopy, the transport gap can be measured by ultraviolet or inverse photoemission spectroscopy and is larger than the optical gap by a quantity equal to the binding energy of the Frenkel excitons.

Fig. 3 shows the temperature dependence of the electric current on pellets for $[Ni(TAAB)(H_2O)_2](C_{14}H_7O_4)_2$, $[Cu(TAAB)(H_2O)_2](C_{14}H_7O_4)_2$ and the complexes from which they were prepared, $[Ni(TAAB)(H_2O)_2](ClO_4)_2$ and $[Cu(TAAB)(H_2O)_2](NO_3)_2$. The variations observed in the magnitude of electric current may be due to the different metallic ions employed: Ni(II) for $[Ni(TAAB)(H_2O)_2](C_{14}H_7O_4)_2$ and Cu(II) for $[Cu(TAAB)(H_2O)_2](C_{14}H_7O_4)_2$. In the former case, the Ni(II) central metallic ion has a basic electronic configuration $3d^8 4s^0 4p^0$ and two unpaired electrons whereas, for the latter compound, the Cu(II) ion has the electronic configuration $3d^9 4s^0 4p^0$ and one unpaired electron. A slight contraction in 3d-orbital size is observed when scanning the transition series, meaning a reduction in 3d-orbital overlap and thus a slightly tighter band in which electrons are more strongly bound to the nuclei, affecting charge transport for $[Cu(TAAB)(H_2O)_2](C_{14}H_7O_4)_2$. Localized charge leads to a long-range Coulomb repulsion which strongly influences the transport of free carriers. Electron–electron interactions result in scattering of the conduction electrons [24].

The electric conductivity σ of these materials, depends on the absolute temperature T as described by the equation

$$\sigma = \sigma_m \exp\left(-\frac{\Delta E_m}{KT}\right) \quad (2)$$

where σ_m is the pre-exponential factor and ΔE_m is the activation energy for electric conductivity; K is Boltzmann's constant. The electric conductivity at 298 K for pellets made of the synthesized molecular solids and the starting materials was also calculated. The results are shown in Table 3. Compound $[Ni(TAAB)(H_2O)_2](C_{14}H_7O_4)_2$ exhibits higher electric conductivity than compound $[Cu(TAAB)(H_2O)_2](C_{14}H_7O_4)_2$ at room temperature. Both materials exhibit a semiconductor-like character that may be due to charge transfer from the anthraflavate anions connecting the anthraflavate oxygen atom with the hydrogen atoms in the water molecules via hydrogen bonds [15]. However, none of them falls within the expected range of electric conductivities for molecular semiconductors (10^{-6}–10^{-1} cm^{-1} Ω^{-1}) [25,26]. This may be explained by the fact that these measurements were performed on pellets, whose electric conductivities are smaller than those obtained in thin films by three to six orders of magnitude. These values, however, are not accurate since pellet thickness is quite large (about 1 mm), so the real trajectory of charge carriers in the material is unknown [25]. The use of films represents a more trustworthy approach when measuring electrical conductivity.

Fig. 4 shows the temperature dependence of electric current through thin films during measurements, for a constant applied voltage in the ohmic regime. It may be concluded that, at low temperatures, $[Ni(TAAB)(H_2O)_2](C_{14}H_7O_4)_2$ shows a slightly larger conductivity than $[Cu(TAAB)(H_2O)_2](C_{14}H_7O_4)_2$, as also happened with

Table 2
Optical parameters measured on thin films

Compound	Refraction index	Reflectance (%)	Optical activation energies E_g (eV)	Activation energies ΔE_m (eV)
$[Ni(TAAB)(H_2O)_2](C_{14}H_7O_4)_2$	1.749	7.4	1.4	0.161
$[Cu(TAAB)(H_2O)_2](C_{14}H_7O_4)_2$	1.897	9.6	2.3	0.0112
$(Ni(TAAB))(ClO_4)_2$	1.268	1.4	2.3	0.057
$(Cu(TAAB))(NO_3)_2$	1.672	6.3	2.0	0.081

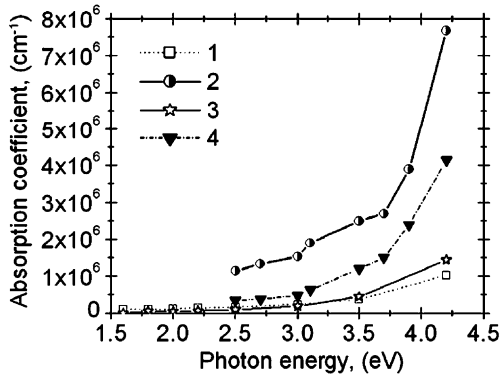

Fig. 2. Absorption coefficient as a function of photon energy for complexes $[Ni(TAAB)(H_2O)_2](C_{14}H_7O_4)_2$ (**1**), $[Cu(TAAB)(H_2O)_2](C_{14}H_7O_4)_2$ (**2**), $[Ni(TAAB)(H_2O)_2](ClO_4)_2$ (**3**) and $[Cu(TAAB)(H_2O)_2](NO_3)_2$ (**4**).

pellet measurements. Current flows in $[Cu(TAAB)(H_2O)_2](C_{14}H_7O_4)_2$ thin films, however, grew faster with increasing temperature values. As the only significant difference between the two compounds is the metallic ion in the coordination sphere, changes in current may be attributed to it [27] and may depend mainly on the number of electrons and their energy levels, on ion and orbital sizes and on the distance between crystallographic planes.

Table 3 shows the electric conductivity results on thin films for the complexes. Although both thin films were rather similar, the one with the highest conductivity at room temperature is $[Ni(TAAB)(H_2O)_2](C_{14}H_7O_4)_2$; the small change may be due again to the central metallic ion. These conductivity values are within the expected range for molecular semiconductor compounds, so these materials may be classified as semiconductors. On the other hand, these materials show a sizable orbital overlap because of the transition-metal d-orbital spatial extent. This is a requirement reported by Simon and Tournillac [26] for molecular semiconductors. Moreover, according to Jircitano and Timken [27], charge transport is provided by the highly ordered structures that are formed in these materials. These structures present preferential directions for electric conduction via the anthraflavate–anion rows that lead to a

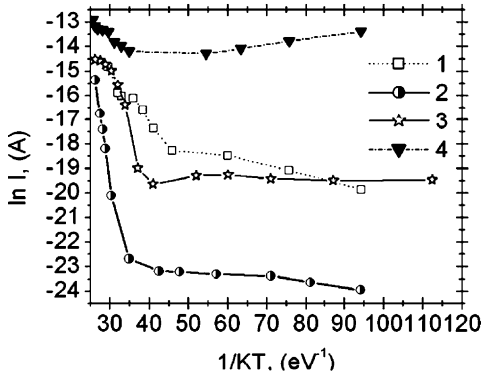

Fig. 3. Electric current as a function of temperature for molecular materials $[Ni(TAAB)(H_2O)_2](C_{14}H_7O_4)_2$ (**1**), $[Cu(TAAB)(H_2O)_2](C_{14}H_7O_4)_2$ (**2**), $[Ni(TAAB)(H_2O)_2](ClO_4)_2$ (**3**) and $[Cu(TAAB)(H_2O)_2](NO_3)_2$ (**4**) in pellet.

Table 3
Pellet and thin-film electrical conductivity at 20 °C (100 V) in the ohmic regime

Compound	Electrical conductivity in pellets, σ (10^{-9} $\Omega^{-1}cm^{-1}$)	Electrical conductivity in thin films, σ (10^{-6} $\Omega^{-1}cm^{-1}$)
$[Ni(TAAB)(H_2O)_2](C_{14}H_7O_4)_2$	0.82	2.7
$[Cu(TAAB)(H_2O)_2](C_{14}H_7O_4)_2$	0.0026	2.1
$(Ni(TAAB))(ClO_4)_2$	1.3	3.5
$(Cu(TAAB))(NO_3)_2$	7.6	3.8

remarkable anisotropic character, which is why they have been called “pseudo-one-dimensional” materials. Room-temperature electric conductivity values for the starting materials (3.5×10^{-6} Ω^{-1} cm^{-1} for nickel compound and 3.8×10^{-6} Ω^{-1} cm^{-1} for copper compound) are higher than those obtained by Jircitano and Timken [27] for their compounds $[M(TAAB)(BF_2)$ and $M(TAAB)(I_2)_{2.7}]$ with M=Pd and Pt ($\sigma=1\times10^{-7}$ Ω^{-1} cm^{-1}).

In amorphous materials, the absence of long-range order leads to the apparition of tails in the energy bands [28]. These tail bands are formed by localized electronic states; they are separated from extended states in the bands by a mobility edge. The electrical activation energy is related to the energy necessary to delocalize charge carriers through electronic transitions from localized states towards extended states. The activation of the intrinsic electrical conductivity in semiconductor-like materials may be also explained by thermal excitation from valence band to conduction band.

In our case, the small difference in conductivity between the thin films may be attributed to the character of the metallic ions employed, considering that nickel-based thin films exhibit higher room-temperature conductivity than copper-based thin films. Furthermore, these compounds show an important orbital overlap probably due to the spatial extension of the transition-metal orbitals as suggested by Simon and Tournillac [26]. On the other hand, Jircitano and Timken [27] reported that charge transfer for molecular materials along particular directions can be

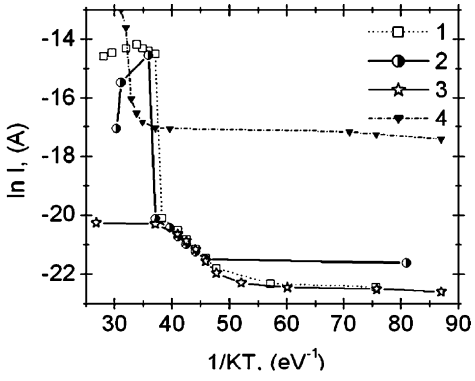

Fig. 4. Electric current as a function of temperature for molecular materials $[Ni(TAAB)(H_2O)_2](C_{14}H_7O_4)_2$ (**1**), $[Cu(TAAB)(H_2O)_2](C_{14}H_7O_4)_2$ (**2**), $[Ni(TAAB)(H_2O)_2](ClO_4)_2$ (**3**) and $[Cu(TAAB)(H_2O)_2](NO_3)_2$ (**4**) in thin film.

related to highly ordered structures. In the compounds that we studied, the anthraflavate anions are joined by hydrogen bonds [15]. Hydrogen bonds in anthraflavate anions can explain charge transfer in these compounds. On the other hand, the anthraflavate anion ribbons surround the tetraaza macrocations to which they join by bonds generated between the oxygen atoms of the quinone anions and the central metallic ion using a water molecule as intermediary [15].

The electrical activation values and optical band gap energies do not show any similarity. This fact may be explained considering that both energies are associated with different phenomena. The calculated ΔE_m values are much lower than those obtained for the optical band gap E_g. The ΔE_m energy is an activation energy involving both the energy necessary to excite electrons from the localized states in the tail band toward extended states through the mobility edge and the electrical conduction by means of the hopping mechanism between localized states. The E_g energy is related to non-direct transitions from valence band to conduction band and is affected by the generation of Frenkel excitons.

4. Conclusion

Thin films containing diaqua tetrabenzo (*b*,*f*,*j*,*n*) {1,5,9,13} tetraazacyclohexadecine copper (II) and nickel (II) bisanthraflavates have been prepared by a vacuum thermal evaporation process. The r.m.s. roughness of the films evaluated by AFM was 40.5 nm for [Ni(TAAB)$(H_2O)_2$]$(C_{14}H_7O_4)_2$ and 68.1 nm for [Cu(TAAB)$(H_2O)_2$]$(C_{14}H_7O_4)_2$. Thin-film morphology seems to depend strongly on the metallic ion in the molecular structure, but without the existence of pinholes. FTIR results show that the evaporation process did not change the chemical composition of the analyzed complexes, [Ni(TAAB)$(H_2O)_2$]$(C_{14}H_7O_4)_2$ and [Cu(TAAB)$(H_2O)_2$]$(C_{14}H_7O_4)_2$. Although the deposited material is amorphous in nature, it is formed by the same chemical unit as those of the synthesized powder. The thermal evaporation process does not change the intra-molecular bonds, suggesting that the deposition process has a molecular nature and the substrate temperature is not high enough to provide the surface mobility necessary for the molecular units to produce crystalline films.

From the electric current values, it is clear that all the molecular thin films show a semiconductor-like behaviour after evaporation. It was also found that the electric current as a function of temperature is always higher for the nickel complexes than for those with copper, which can be explained by the different electronic configuration of the central metallic ion. Thin films show higher electric conductivity values than pellets.

The availability of thin films made from the materials studied in this work, their calculated optical band gap and the order of magnitude of their electrical conductivity seem to make it possible their consideration for electronic-device applications.

Acknowledgment

This work was supported by CONACYT project number J36715-U (Mexico).

References

[1] F.L. Carter, R.E. Siatokowski, H. Wohltjen, Molecular Electronic Devices, North Holland, New York, 1988, p. 1.
[2] F. Garnier, G. Horrowitz, X. Peng, D. Fichou, Adv. Mater. 2 (1990) 592.
[3] P. Cassoux, D. De Caro, L. Valade, H. Casellas, B. Daffos, M.E. Sánchez Vergara, Mol. Cryst. Liq. Cryst. 380 (2002) 45.
[4] J. Caro, S. Garelik, A. Figeras, Chem. Vap. Depos. 2 (1996) 251.
[5] A. Figueras, S. Garelik, J. Caro, J. Cifre, J. Venciana, C. Rovira, E. Ribera, E. Canadell, A. Seffar, J. Cryst. Growth 166 (1996) 798.
[6] P. Cassoux, D. De Caro, L. Valade, H. Casellas, B. Daffos, M.E. Sánchez Vergara, Mol. Cryst. Liq. Cryst. 380 (2002) 45.
[7] A.J. Epstein, S. Etemad, A.F. Garito, A.J. Heeger, Phys. Rev., B Condens. Matter 5 (1972) 952.
[8] L.B. Coleman, M.J. Cohen, D.J. Sandman, F.G. Yamagishi, A.F. Garito, A. Ferraris, Solid State Commun. 12 (1973) 1125.
[9] K. Soo-Jong, M. Michiko, S. Kiyotaka, J. Porphyr. Phthalocyanines 4 (2000) 136.
[10] B.N. Duncan, L. Inabe, N.K. Jaggi, J.W. Lyding, O. Schender, M. Hanack, C.R. Kanneworf, T.J. Marks, L.H. Schwatz, J. Am. Chem. Soc. 106 (1984) 3207.
[11] H. Kobayashi, A. Kobayashi, P. Cassoux, Chem. Soc. Rev. 29 (2000) 325.
[12] J. Labuda, V. Plaskoñ, Inorg. Chim. Acta 13 (1988) 146.
[13] L.I. Smith, J.W. Opie, Org. Synth. 11 (1948) 28.
[14] B. Douglas, Inorganic Syntheses, vol. XVIII, Wiley Interscience, Hoboken, New Jersey, 1968, p. 1.
[15] M.E. Sánchez-Vergara, J. Gómez-Lara, R.A. Toscano, S. Hernández-Ortega, J. Chem. Crystallogr. 28 (1998) 825.
[16] M. Sridharan, S.K. Narayandass, D. Mangalaraj, J. Mater. Sci., Mater. Electron. 13 (2002) 471.
[17] J. Tauc, in: F. Abeles (Ed.), Optical Properties of Solids, North-Holland Publishing Co., Amsterdam, 1972, p. 277.
[18] R.K. Mane, B.D. Ajalkar, P.N. Bhosale, Mater. Chem. Phys. 82 (2003) 534.
[19] F. Urbach, Phys. Rev. 92 (1953) 1434.
[20] S. Adachi, Optical Properties of Crystalline and Amorphous Semiconductors, Kluwer Academic Publishers, Boston, 1999, p. 1.
[21] G.D. Cody, in: J.I. Pankove (Ed.), Hydrogenated Amorphous Silicon, Part B: Optical Properties, Semiconductors and Semimetals, vol. 21, Academic Press, Orlando, 1984.
[22] G. Burns, Solid State Physics, Academic Press Inc., San Diego, 1990.
[23] I.G. Hill, A. Kahn, Z.G. Soos, R.A. Pascal Jr., Chem. Phys. Lett. 327 (2000) 181.
[24] A. Brau, J.P. Farges, in: Jean-Pierre Fargas (Ed.), Organic Conductors, Marcel Dekker, Inc., New York, 1994.
[25] A. Ortiz-Rebollo, V. García-Montalvo, J. Gómez-Lara, M.E. Sánchez-Vergara, J. Coord. Chem. 54 (2001) 441.
[26] J. Simon, F. Tournillac, New J. Chem. 11 (1997) 383.
[27] A.J. Jircitano, M.D. Timken, K. Bowman, J.R. Ferrano, J. Am. Chem. Soc. 101 (1979) 7761.
[28] J. Metz, M. Hanack, J. Am. Chem. Soc. 105 (1983) 828.